

Highly Active and Selective Platinum(II)-Catalyzed Isomerization of Allylbenzenes: Efficient Access to (*E*)-Anethole and Other Fragrances via Unusual Agostic Intermediates

Alessandro Scarso,^{*,†} Marco Colladon,[†] Paolo Sgarbossa,[‡] Claudio Santo,[†]
Rino A. Michelin,[‡] and Giorgio Strukul^{*,†}

[†]Dipartimento di Chimica, Università Ca' Foscari di Venezia, Dorsoduro 2137, 30123 Venezia, Italy, and

[‡]Dipartimento di Processi Chimici dell'Ingegneria, Università di Padova, Via Marzolo 9, 35131 Padova, Italy

Received January 12, 2010

Terminal alkene isomerization reactions can be efficiently catalyzed by Pt^{II} complexes bearing a chelating diphosphine and an alkyl or, better, aryl moiety under mild experimental conditions. In particular diphosphines, such as dppb, characterized by a large bite angle in conjunction with a pentafluorophenyl residue coordinated to Pt enable quantitative conversion of the reagent into internal alkenes within few hours at 50 °C in CHCl₃ as solvent. *E/Z* selectivity can be as high as 98:2 for allylbenzene, and the catalytic system can be fruitfully applied to the preparation of *E* fragrances derived by isomerization of substituted allylbenzene derivatives. The selectivity increases during the progress of the reaction because of a subsequent catalytic step where the *Z* alkene coordinates to the Pt and is converted into the *E* isomer. NMR investigation on the catalyst showed formation of agostic Pt···H intermediate species derived by insertion of the substrate into the Pt–aryl bond followed by β-hydride elimination. Formation of such agostic species is promoted by the steric hindrance imparted by the diphosphine characterized by a large bite angle. Kinetic studies and DFT calculations on the possible agostic intermediates shed light on their structure and enable the formulation of a possible catalytic mechanism.

Introduction

Alkene isomerization is an important atom-efficient reaction fulfilling both sustainability criteria and widespread applications in industry.¹ In fact, it is mainly used for the synthesis of commodities such as linear olefins in the SHOP process or adiponitrile preparation from butadiene and HCN, where two isomerization steps are involved, or in vinylnorbornene isomerization to provide ethylenenorbornene, a useful comonomer for elastomer production.²

This reaction is also largely employed in the synthesis of pharmaceuticals and fine chemicals such as fragrances.^{3–5} Noteworthy examples are (i) 6-methyl-6-hepten-2-one isomerization in BASF vitamin A synthesis,⁶ (ii) the asymmetric allylamine isomerization from myrcene in the (–)-menthol

synthesis mediated by chiral Rh catalyst developed by Noyori,⁷ and (iii) the industrial isomerizations of allyl benzene derivatives such as estragole, eugenol, and safrole to the corresponding internal alkenes used as fragrances, where high productivity as well as high selectivity for the *E* isomer are important challenges.² In the latter process, *E* products are marketed, while *Z* isomers are characterized by an unpleasant taste and in some cases a toxic character, requiring a lower than 1% content for human use. At present, tedious purification steps are required to isolate the *E* isomer, thus causing an increasing interest in the development of highly selective isomerization processes in order to decrease production costs as well as avoid the stoichiometric use of bases. Currently, industrial isomerization of estragole to *E*-anethole is performed with KOH at high temperatures (200 °C) with moderate yields of about 56% and *E/Z* selectivities of 82:18, while most fragrances reported above are still obtained by extractions from natural sources with an overall annual production of several million metric tons.⁸

The catalysts developed for terminal alkene isomerization are numerous. Heterogeneous ones are preferred for industrial applications and rely on solid bases whose activity is related to the ability to deprotonate the substrate, thus providing a carbanion isomerizing into thermodynamically

*Corresponding authors. E-mail: alesca@unive.it; strukul@unive.it. Fax: +39-0412348517.

(1) van Leeuwen P. W. N. M. *Homogeneous Catalysis*; Kluwer Academic Publishers: Dordrecht, 2004; pp 101–105.

(2) Parshall G. W.; Ittel S. D. *Homogeneous Catalysis*, 2nd ed.; Wiley: New York, 1992; pp 9–24.

(3) Cornils B.; Herrmann W. A. *Applied Homogeneous Catalysis with Organometallic Compounds*; Wiley: New York, 2002; pp 980–991.

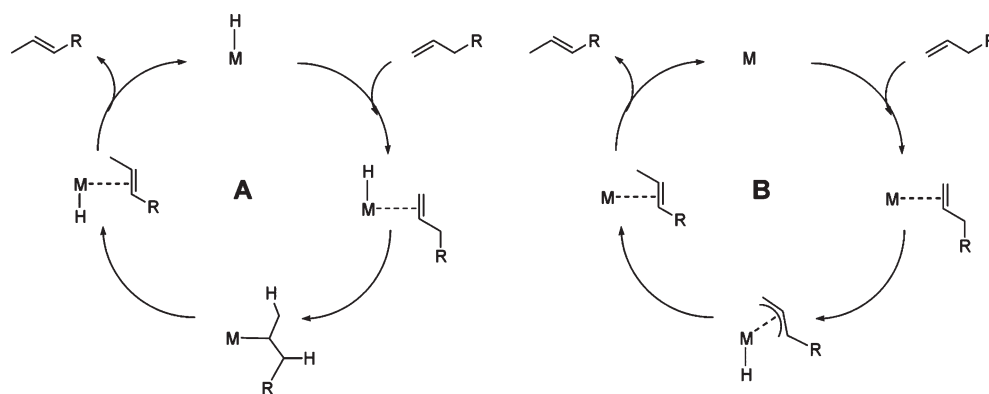
(4) (a) Bauer K.; Garbe D.; Surburg H. *Common Fragrance and Flavour Materials*, 4th ed.; Wiley: New York, 2001; pp 171–226. (b) Kraft P.; Swift K. A. D. *Current Topics in Flavour and Fragrance Research*; Swift, K. A. D., Ed.; VHC, Zürich, Switzerland, and Wiley-VCH Verlag GmbH, Weinheim, Germany, 2008.

(5) Chapuis, C.; Jacoby, D. *Appl. Catal. A* **2001**, *221*, 93–117.

(6) Pommer, H.; Nurrenbach, A. *Pure Appl. Chem.* **1975**, *43*, 527–552.

(7) Inoue, S.-I.; Takaya, H.; Tani, K.; Otsuka, S.; Sato, T.; Noyori, R. *J. Am. Chem. Soc.* **1990**, *112*, 4897–4905.

(8) Sharma, S. K.; Srivastava, V. K.; Jasra, R. V. *J. Mol. Catal. A* **2006**, *245*, 200–209.

Scheme 1. Terminal Alkene Isomerization Reaction via (A) 1,2-Hydrogen Shift and (B) 1,3-Hydrogen Shift

more stable internal alkenes.⁹ Such solid catalysts are usually active at high temperatures (>200 °C) and are critically affected by the presence of water. A different approach applies to homogeneous isomerization catalysts, generally transition metal complexes operating via two possible main pathways (Scheme 1):² (A) hydride addition elimination mechanism (1,2-hydrogen shift) and (B) π -allyl mechanism (1,3-hydrogen shift). By virtue of the π -allyl intermediate, mechanism B may have a dramatic effect on the *E/Z* ratio, providing high amounts of the *E* isomer, which is favored both kinetically and thermodynamically.¹⁰

Metal centers capable of catalyzing alkene isomerization span from Ti² and Fe² to softer Lewis acidic ones such as Rh,¹¹ Ru,^{8,12} Ir,¹³ Pd,^{14,15,12b} and Ni.¹⁶ The latter class, albeit more expensive, is generally more productive.

During our endeavor on Pt^{II} oxidation reactions with H₂O₂ using electron-poor complexes as catalysts¹⁷ we observed partial alkene isomerization during epoxidation that prompted us to investigate more deeply the reaction. Herein we report the results observed in the selective isomerization of alkenes for the achievement of fragrances under mild

experimental conditions, mediated by the electron-poor cationic Pt^{II} complexes shown in Chart 1, together with some mechanistic investigations and DFT calculations that evidenced for the first time the involvement of agostic species as key intermediates in the isomerization process.

Results and Discussion

The Catalysts. Most of the complexes tested as catalysts in the isomerization reaction have already been reported elsewhere (see Experimental Section). **1**, **2**, **3**, **5**, and **6** are new complexes, and they have been synthesized in good yields by halide abstraction from the corresponding Pt–Cl derivatives according to the procedure reported in the Experimental Section. As shown in Chart 1, all catalysts are cationic Pt^{II} (or Pd^{II} in one case) soft Lewis acids containing a diphosphine (or two *trans* monophosphines in **5**) in which the P–Pt–P bite angle was varied by changing the length of the aliphatic chain linking the two phosphorus atoms, along with an alkyl or aryl ligand (substituted or unsubstituted), to modify both the electronic and steric properties of the complex and finally a labile and easily displaceable water molecule.

Isomerization of Allylbenzene. The activities of the catalysts in the selective isomerization of allylbenzene to the corresponding *E* and *Z* isomers (Scheme 2), chosen as a model substrate, are reported in Table 1. It should be emphasized that the isomerization of this substrate as well as the other ones reported in this work can be carried out in air with no need for purified, dry solvents. Complex **1** showed interesting activity toward allyl benzene with almost complete conversion after 24 h with an *E/Z* ratio of 87:13, which remained almost constant during the reaction progress. Substitution of the methyl residue with a more electron-withdrawing trifluoromethyl group like in **2** caused a substantial increase in activity and, more interestingly, a marked increase in selectivity for the *E* isomer, with the *E/Z* value growing to 95:5 during the reaction progress.

The increase of the *E/Z* value during the reaction progress is observed also with catalysts **4b** and **4bPd** and might be indicative of either an evolution of the catalytically active species or the existence of a consecutive reaction. The presence of an aryl residue on the complex as in **3** induces a further enhancement of catalytic activity with complete conversion in only 5 h and an *E/Z* value of 95:5. Again, replacement of the aryl residue with a more electron-withdrawing pentafluorophenyl residue as in **4e** led to an even better catalyst with complete conversion in only 2 h and *E/Z* selectivity of 97:3.

(9) (a) Kishore, D.; Kannan, S. *Green Chem.* **2002**, *4*, 607–610. (b) Srivastava, V. K.; Bajaj, H. C.; Jasra, R. V. *Catal. Commun.* **2003**, *4*, 543–548. (c) Kishore, D.; Kannan, S. *J. Mol. Catal. A* **2004**, *223*, 225–230. (d) Kishore, D.; Kannan, S. *App. Catal. A* **2004**, *270*, 227–235. (e) Kishore, D.; Kannan, S. *J. Mol. Catal. A* **2006**, *244*, 83–92.

(10) Tuner, M.; Jouanne, J. V.; Brauer, H.-D.; Kelm, H. *J. Mol. Catal.* **1979**, *5* (425), 433–447.

(11) (a) Morrill, T. C.; D'Souza, C. A. *Organometallics* **2003**, *22*, 1626–1629. (b) Yan, Y.; Zhang, X.; Zhang, X. *J. Am. Chem. Soc.* **2006**, *128*, 16058–16061. (c) Tan, K. L.; Bergman, R. G.; Ellman, J. J. *Am. Chem. Soc.* **2002**, *124*, 13964–13965.

(12) (a) Schmidt, B. *Chem. Commun.* **2004**, 742–743. (b) Sharma, S. K.; Srivastava, V. K.; Pandya, P. H.; Jasra, R. V. *Catal. Commun.* **2005**, *6*, 205–209. (c) Hanessian, S.; Giroux, S.; Larsson, A. *Org. Lett.* **2006**, *8*, 5481–5484. (d) Courchay, F. C.; Sworen, J. C.; Ghiviriga, I.; Abboud, K. A.; Wagener, K. B. *Organometallics* **2006**, *25*, 6074–6086. (e) Yue, C. J.; Liu, Y.; He, R. *J. Mol. Catal. A* **2006**, *259*, 17–22. (f) Krompiec, S.; Kuźnik, N.; Urbala, M.; Rzepa, J. *J. Mol. Catal. A* **2006**, *248*, 198–209. (g) Donohoe, T. J.; O'Riordan, T. J. C.; Rosa, C. P. *Angew. Chem.* **2009**, *121*, 1032–1035. *Angew. Chem., Int. Ed.* **2009**, *48*, 1014–1017; (h) Erdogan, G.; Grotjahn, D. B. *J. Am. Chem. Soc.* **2009**, *131*, 10354–10355.

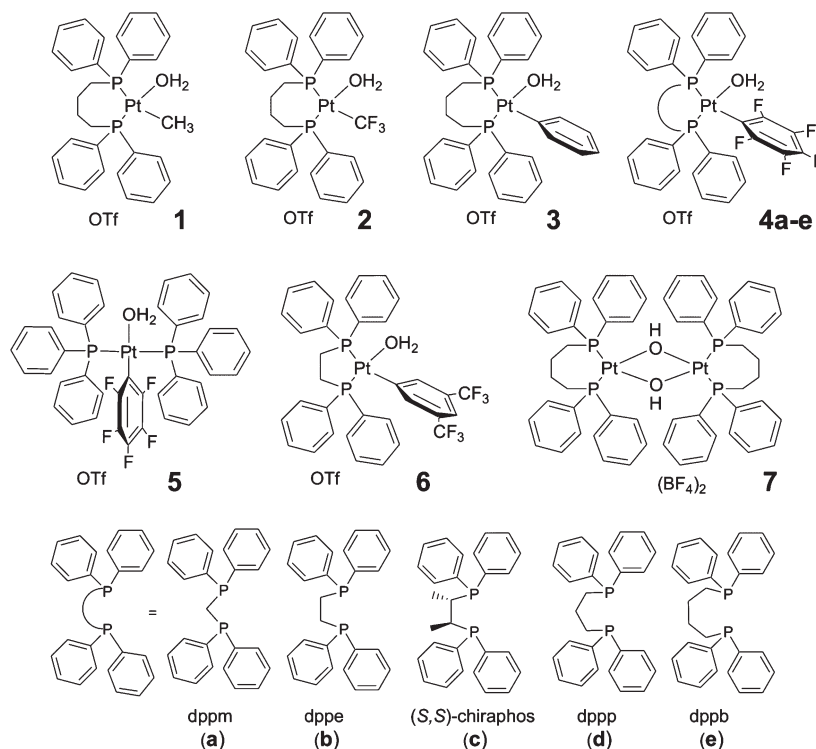
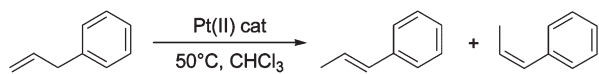
(13) Baxendale, I. R.; Lee, A.-L.; Ley, S. V. *J. Chem. Soc., Perkin Trans. 1* **2002**, 1850–1857.

(14) Jennerjahn, R.; Piras, I.; Jackstell, R.; Franke, R.; Wiese, K.-D.; Beller, M. *Chem.—Eur. J.* **2009**, *15*, 6383–6388.

(15) Kim, I. S.; Dong, G. R.; Jung, Y. H. *J. Org. Chem.* **2007**, *72*, 5424–5426.

(16) Zhang, J.; Gao, H.; Ke, Z.; Bao, F.; Zhu, F.; Wu, Q. *J. Mol. Catal. A* **2005**, *231*, 27–34.

(17) (a) Colladon, M.; Scarso, A.; Sgarbossa, P.; Michelin, R. A.; Strukul, G. *J. Am. Chem. Soc.* **2006**, *128*, 14006–14007. (b) Colladon, M.; Scarso, A.; Sgarbossa, P.; Michelin, R. A.; Strukul, G. *J. Am. Chem. Soc.* **2007**, *129*, 7680–7689. (c) Pizzo, E.; Sgarbossa, P.; Scarso, A.; Michelin, R. A.; Strukul, G. *Organometallics* **2006**, *25*, 3056–3062.

Chart 1. Pt^{II} Complexes Investigated As Catalysts for Alkene IsomerizationScheme 2. Allyl Benzene Isomerization to internal *E* and *Z* Alkenes Mediated by Pt^{II} Catalysts

Spurred by the interesting results observed with complex **4e**, we decided to explore the effect of different ligands on the activity and selectivity of the reaction. **4a** showed low activity and selectivity, while both properties increased with **4b**, characterized by a larger bite angle. Notably, the flexibility of the diphosphine ligand seems to positively influence activity, as observed by comparison with complex **4c**, a more rigid analogue of **4b**, the latter showing a higher catalytic activity. An even larger bite angle (complex **4e**) caused a further increase in activity. While Lewis acidity seems a common requirement with respect to epoxidation of terminal alkenes with the same class of complexes,¹⁷ an opposite trend is observed with respect to the diphosphine bite angle, as in epoxidation larger bite angles reduce activity because of steric congestion around the vacant site arising from water displacement. It is interesting to notice that while activity is strongly influenced by the bite angle of the diphosphine, much lower is the influence on stereoselectivity (see complex **4a** vs **4d**). The *cis* coordination of the bidentate ligands is another important issue as observed by comparison with complex **5**, bearing two *trans* triphenyl phosphine ligands, showing very low catalytic activity. Substitution with a more bulky electron-withdrawing group as in **6** caused a dramatic decrease in activity and also a very low selectivity (see **4b**) probably due to a difficult approach of the alkene to the complex. The Pd^{II} complex **4b-Pd**, structurally analogous to Pt^{II} **4b**, unexpectedly showed a lower activity. Dimeric species **7**, where upon dissociation only one coordination site is available for alkene coordination, provided the isomerized products with very low activity but good selectivity.

Table 1. Catalytic Isomerization of Allyl Benzene with Pt^{II} Catalysts: Catalyst Screening^a

catalyst	time (h)	yield (%)	<i>E</i> : <i>Z</i> (%)
none	16	0	
1 , [(dppb)Pt(CH ₃)(H ₂ O)]OTf	1	8	90:10
	3	20	87:13
	24	96	86:14
2 , [(dppb)Pt(CF ₃)(H ₂ O)] OTf	2	11	75:15
	4	41	81:19
	24	99	95:5
3 , [(dppb)Pt(C ₆ H ₅)(H ₂ O)] OTf	1	19	94:6
	3	85	95:5
	5	99	95:5
4a , [(dppm)Pt(C ₆ F ₅)(H ₂ O)]OTf	24	22	89:11
4b , [(dppe)Pt(C ₆ F ₅)(H ₂ O)]OTf	2	30	62:38
	24	99	93:7
4c , [(S,S-Chiraphos)Pt(C ₆ F ₅)(H ₂ O)]OTf	2	14	80:20
	24	91	80:20
4d , [(dppp)Pt(C ₆ F ₅)(H ₂ O)]OTf	2	16	92:8
	24	99	92:8
4e , [(dppb)Pt(C ₆ F ₅)(H ₂ O)]OTf	2	99	97:3
4b-Pd , [(dppe)Pd(C ₆ F ₅)(H ₂ O)]OTf	4	6	83:17
	24	27	94:6
5 , <i>trans</i> -[(PPh ₃) ₂ Pt(C ₆ F ₅)(H ₂ O)]OTf	24	21	96:4
6 , [(dppe)Pt(C ₈ H ₃ F ₆)(H ₂ O)]OTf	24	22	51:49
7 , [(dppb)Pt(μ-OH)] ₂ (BF ₄) ₂	5	5	95:5
	24	25	95:5

^a Experimental conditions: [sub]₀ = 0.83 M, cat. 2% mol, solvent chloroform 0.5 mL, *T* 50 °C. Yield determined by GC analysis; dr and product assignment determined by ¹H NMR analysis.

With **4e** as the best catalyst at hand, we investigated the effect of catalyst loading and solvent on the model isomerization reaction. In Table 2 are reported the results for experiments performed with decreasing amounts of complex **4e**. With a loading of < 1% mol the reaction is complete in 4 h still with good selectivity, while with 0.2% activity is obviously negatively affected, while selectivity at high conversion does not appear to be significantly influenced.

Table 2. Catalytic Isomerization of Allyl Benzene with [(dppb)Pt(C₆F₅)(H₂O)](OTf) **4e: Optimization of the Experimental Conditions^a**

conditions	time (h)	yield (%)	TON	<i>E</i> : <i>Z</i> (%)
sub/cat. 50:1, CHCl ₃	2	99	50	97:3
sub/cat. 108:1, CHCl ₃	2	69	75	84:16
	4	99	107	95:5
sub/cat. 500:1, CHCl ₃	4	10	50	83:17
	52	95	475	92:8
sub/cat. 108:1, DCE	4	50	54	80:20
	24	99	107	98:2
sub/cat. 108:1, THF	4	34	37	61:39
	24	91	98	67:33
sub/cat. 108:1, toluene	4	73	79	72:28
	24	99	107	82:18

^a Experimental conditions: [sub]₀ = 0.81 M, solvent 0.5 mL, *T* 50 °C. Yield determined by GC analysis; dr and product assignment determined by ¹H NMR analysis.

Table 3. Substrate Scope in the Catalytic Isomerization of Terminal Alkenes with **4e in CHCl₃ at 50 °C^a**

#	Substrate	Product	Time (h)	Yield (%)	<i>E</i> : <i>Z</i> (%)
1			4	99	95:5
			4	57	97:3
2			12	99	97:3
3			4	29	63:37
			24	54	63:37
4			4	31	77:23
			24	38	77:23
5			4	24	64:36
			24	60	64:36
6			4	9	n.d.
			8	17	n.d.
7			4	18	0:100
			24	45	0:100
8			4	42	-
			24	97	-

^a Experimental conditions: [sub]₀ = 0.81 M, **4e** 1% mol, solvent chloroform 0.5 mL, *T* 50 °C. Yield determined by GC analysis; diastereoselective ratio (*E*/*Z*) and product assignment determined by ¹H NMR analysis.

Reactivity is enhanced in aromatic solvents and decreased in polar THF probably because of solvent competition for coordination to Pt^{II}, while selectivity is positively influenced by chlorinated solvents with an *E*/*Z* ratio up to 98:2 in dichloroethane (DCE).

Scope of the Reaction. In order to investigate the scope of the reaction, we tested catalyst **4e** in CHCl₃ with several terminal alkenes (Table 3). In particular the class of allyl benzene derivatives that are industrially important substrates for the production of fragrances⁴ showed good performance with activities higher than known homogeneous and heterogeneous systems. The selectivity for estragole (allyl-*p*-methoxybenzene, entry 2) as substrate is one of the highest ever reported with good conversions under much milder experimental conditions with respect to known examples.^{12f} Similarly, isomerization of eugenol (entry 4), 3,4-dimethoxyallylbenzene (entry 3), and safrole (entry 5)

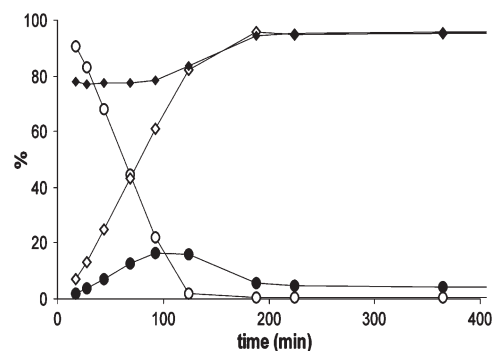
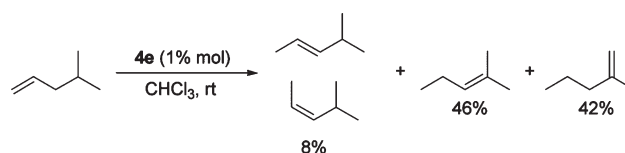


Figure 1. Allyl benzene isomerization with **4e** (2% mol) at 50 °C, [sub] = 0.83 M. (◇) (1*E*)-prop-1-en-1-ylbenzene, (●) (1*Z*)-prop-1-en-1-ylbenzene, (○) allylbenzene, (◆) selectivity to (1*E*)-prop-1-en-1-ylbenzene.

Scheme 3. Isomerization of 4-Methylpentene with **4e in CHCl₃ at Room Temperature**

is characterized by better activities and comparable selectivities to other well-studied homogeneous systems.¹²

As already evidenced by the above substrates, the catalyst is sensitive to the presence of donor heteroatoms; in fact allyl acetate, allyl imidazole, and allyl ethyl ether were unreactive because of competitive coordination by the heteroatoms on the Pt^{II} center. Only allyl phenyl ether was active due to the intrinsically lower Lewis basic character of the oxygen atom of the substrate, as observed for all the other methoxy aryl substrates investigated, although it unexpectedly led to complete stereoselection for the *Z* isomer¹⁸ (Table 3).

Isomerization of terminal acyclic alkenes is very fast with **4e** even at room temperature, but the reaction does not stop at the 2-alkene products, as double-bond migration occurs until thermodynamic distribution¹⁹ is reached, leading to a complex mixture of products as illustrated in Scheme 3. Analogously isomerization of 2-allylcyclohexanone did not show the formation of 2-alkenes; only the conjugated enone was observed, indicative of sequential double-bond migration (entry 6, Table 3). These results clearly evidence that the activity of Pt^{II} complexes toward alkenes²⁰ is better for terminal olefins, but it is good also for internal²¹ and sterically hindered ones.

The reaction profiles in the isomerization of allylbenzene with the complexes reported in Table 1 were analyzed, and an example is reported in Figure 1 for complex **4e**. As can be seen, after a short induction time, both isomerized alkenes start being produced with an initially constant selectivity. Then, as the substrate is depleted, the *Z* product, after

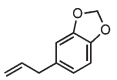
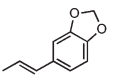
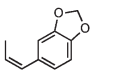
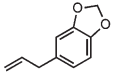
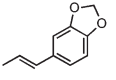
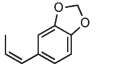
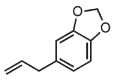
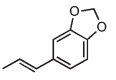
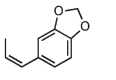
(18) Brett Runge, M.; Mwangi, M. T.; Bowden, N. B. *J. Organomet. Chem.* **2006**, *691*, 5278–5288.

(19) Grimme, S.; Steinmetz, M.; Korth, M. *J. Org. Chem.* **2007**, *72*, 2118–2126.

(20) Sivaramakrishna, A.; Su, H.; Moss, J. R. *Organometallics* **2007**, *26*, 5786–5790.

(21) Pt(II)-catalyzed 1-hexene isomerization as side reaction: Karshedt, D.; Bell, A. T.; Don Tilley, T. *J. Am. Chem. Soc.* **2005**, *127*, 12640–12646.

Table 4. Energy Values for the Different Alkene Isomers Calculated for Allylbenzene and Safrole

Temp (°C)	Alkene Energy (Kcal/mol)		
0	 7.74	 0	 2.84
	 8.12	 0	 3.08
25	 6.58	 0	 3.39
	 6.68	 0	 3.17
50	 6.59	 0	 3.41
	 6.68	 0	 3.21

reaching a maximum concentration, is converted into the *E* isomer in a consecutive isomerization process. This behavior is typical even if it can be more or less evident depending on the individual Pt^{II} catalyst and explains why in Tables 1–3 high selectivities to the *E* isomer occur only at high conversions.

Some DFT calculations on allylbenzene and safrole and their respective isomers have been carried out in order to evaluate the thermodynamic composition at the equilibrium of the different alkenes. The energy values at three different temperatures are reported in Table 4. As can be seen, a moderate decrease in energy difference is observed with temperatures between the terminal alkenes and the internal ones, while the latter show little difference. At 50 °C, i.e., the temperature of the catalytic experiments, and for both substrates considered the *E*-2 isomers are about 6.6 kcal/mol more stable with respect to the corresponding terminal alkene and 3.2–3.4 kcal/mol more stable with respect to the corresponding *Z*-2 isomers. This corresponds to an approximate population of 0% terminal, 99% *E*-2, and 1% *Z*-2 alkene, indicating that in Figure 1 the initial selectivity corresponds to a kinetic control on the terminal to internal isomerization step, while the final selectivity approaches the thermodynamic one.

In Situ NMR Studies. In order to shed light on the reaction pathway and understand the nature of possible reaction intermediates, we performed some NMR experiments where ¹H and ³¹P spectra of the system were recorded during the reaction progress under conditions identical to those reported in Table 1 for the catalytic experiments in order to monitor product formation as well as catalyst speciation. With complex **4e** as the catalyst and allylbenzene as the substrate the ¹H NMR spectrum of the system did not show

the presence of any Pt–H species, which usually have resonances at very high fields ($\delta < 0$ ppm). At the same time, the ³¹P resonances typical of **4e** tend to decrease after a few catalytic cycles (5 min, 2% yield in internal alkenes), and the formation of a new species is observed, characterized by the presence of two P resonances (18.3 ppm, ¹J_{P–Pt} 5266 Hz, and 14.9 ppm, ¹J_{P–Pt} 3156 Hz) both without Pt–F coupling constants indicative of the loss of the pentafluoro phenyl residue (Figure 2A). At the same time, GC-MS analysis showed the presence of traces of pentafluoroaryl-alkenes, confirming the cleavage of the Pt–C₆F₅ bond and coupling of the fluorinated organic residue with the substrate. After 40 min only the new species was present, which remained unchanged until reaction reached completeness. With *p*-methoxy-allylbenzene a similar behavior occurred with disappearance of **4e** signals and formation of the new species similar to the one observed with allylbenzene (Figure 2B).

Spectroscopic analysis allowed describing such species as unusually stable Pt^{II}-alkyl complexes with Pt···H agostic interactions,²² justified by the exceptionally high ¹J_{P–Pt} coupling constant²³ and forced by the steric hindrance imparted in this case by the dppb ligand. Attempts to observe agostic interactions on ¹H NMR in the upfield region of the spectrum at very low temperature (down to 168 K)²² were unsuccessful probably because of overlap of such signals with those belonging to the substrate and products of the isomerization reactions present in much higher concentrations. This weak interaction arises when sterically congested ligands with large bite angles surround Pt-alkyl species, bringing the H atom in close contact with the Pt metal center. Interestingly, upon increasing benzene ring substitution as in 3,4-dimethoxyallylbenzene, eugenol, and safrole as substrates, two new species were present, both characterized by one large (~5000 Hz) and one small (~3000 Hz) ¹J_{P–Pt} in 27:73, 25:75, and 45:55 ratios, respectively (Figure 2C, D, and E). The chemical shifts and coupling constants observed for such species are substrate sensitive and were found to be fully in agreement with the formation of diphosphine platinum-alkyl complexes with agostic Pt···H interaction.²²

The rate of catalyst evolution during the reaction progress and the presence of agostic intermediate species as resting states are most likely induced by the steric hindrance imparted by the ligand. This also explains the reactivity differences observed for homologous complexes **4a–e** (Table 1), which differ in the bite angle of the diphosphine on going from dpdm to dppb.

Agostic Pt···H species are detected also for other catalysts bearing the dppb diphosphine ligand as in **1**, **2**, and **3**. An analogous ³¹P NMR investigation was performed on catalysts **1**, **2**, and **3**, and in all cases agostic species (Scheme 4) were present as minor species, while their formation was slower compared to **4e** depending on the alkyl (aryl) ligand according to the order –CH₃ < –CF₃ < –C₆H₅ < –C₆F₅, in agreement with the effects on Lewis acidity^{17c} and catalyst activity already observed in Table 1. The reactivity order observed for catalysts bearing different alkyl- and aryl-coordinated moieties seems in general agreement with the

(22) (a) Carr, N.; Dunne, B. J.; Mole, L.; Orpen, A. G.; Spencer, J. L. *J. Chem. Soc., Dalton Trans.* **1991**, 863–871. (b) Carr, N.; Mole, L.; Orpen, A. G.; Spencer, J. L. *J. Chem. Soc., Dalton Trans.* **1992**, 2653–2662. (c) Spencer, J. L.; Mhinzi, G. S. *J. Chem. Soc., Dalton Trans.* **1995**, 3819–3824.

(23) Mullen, C. A.; Gagne, M. R. *J. Am. Chem. Soc.* **2007**, *129*, 11880–11881.

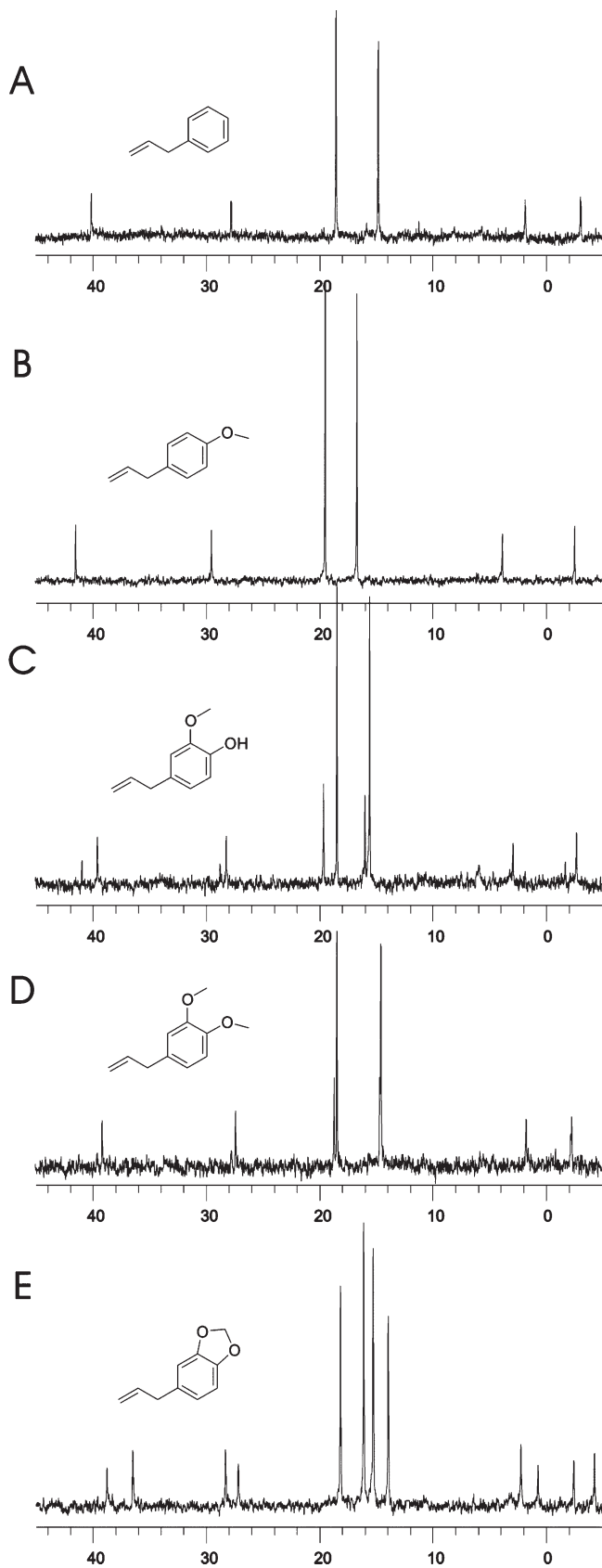
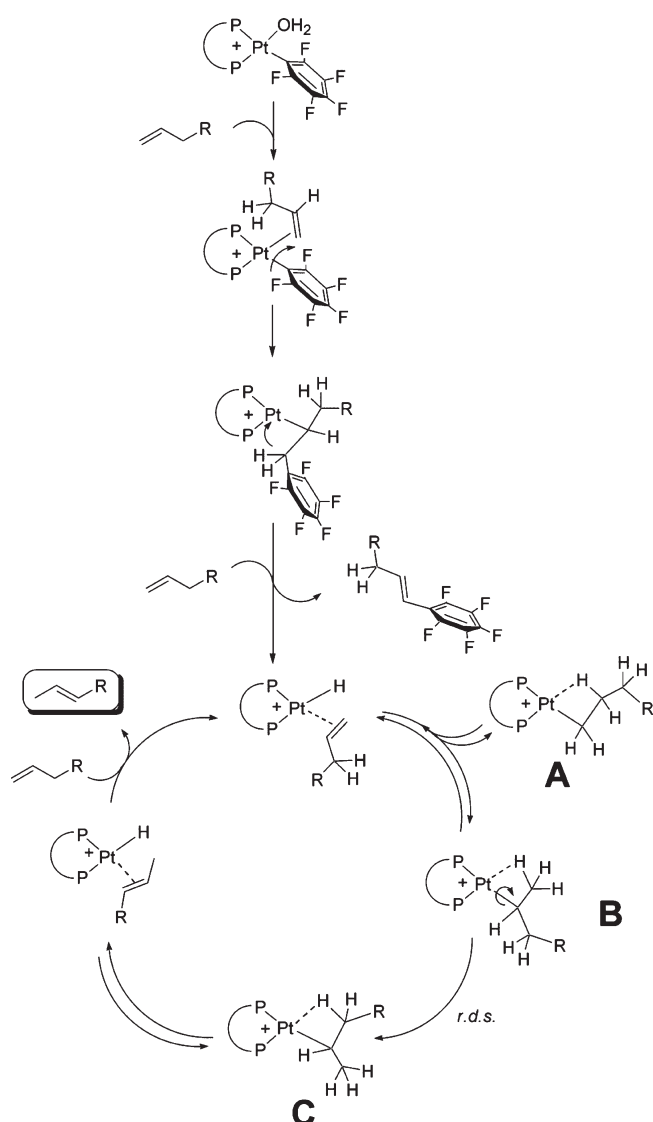


Figure 2. ^{31}P spectra of agostic intermediate species arising from **4e** and (A) allylbenzene, (B) *p*-methoxy-allylbenzene, (C) eugenole, (D) 3,4-dimethoxy-allylbenzene, and (E) safrole.

strength of the Pt–C bond, as confirmed by the increasing Pt– $\text{P}_{\text{C-trans}}$ coupling constants (**1** 1849 Hz, **2** 1904 Hz, **4e**

Scheme 4. Proposed Isomerization Pathway



2136 Hz), even though for **3** (1757 Hz) the Pt– $\text{P}_{\text{C-trans}}$ is smaller probably due to enhanced back-bonding ability.

After reaction completion the remaining Pt^{II} species observed for **1**, **2**, **3**, and **4e** was mainly $[\text{Pt}(\text{dppb})(\mu\text{-OH})_2]^{2+}$ (δ 3.3 ppm, $J_{\text{P-Pt}}$ 3530 Hz), formed by interaction with trace water, which is only sparingly active toward terminal allyl benzene isomerization (25% of conversion with *E/Z* 95:5 after 24 h in the same experimental conditions as in Table 1).

Possible Reaction Pathway. The reaction profile shown in Figure 1 clearly indicates that in the isomerization of allylbenzene with **4e** the decay of substrate is independent of its concentration, allowing the determination of the reaction rate very accurately. This behavior is general, although the extent of the induction time, which in the case of **4e** is very short, can vary depending on catalyst nature and concentration. In order to gain more insight into the mechanism, the effect of **4e** concentration in the same reaction was determined. This is reported in Figure 3 and shows that the reaction is first-order on initial catalyst concentration. No reaction is observed in the absence of catalyst, and for concentrations above 2×10^{-2} M the catalyst becomes incompletely soluble in the reaction medium.

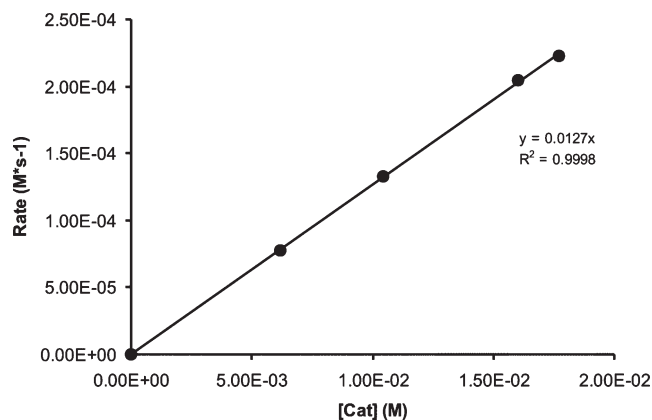


Figure 3. Effect of the concentration of **4e** on the rate of isomerization of allylbenzene. Experimental conditions: $[\text{sub}]_0 = 0.83 \text{ M}$, solvent chloroform 0.5 mL , $T 50 \text{ }^\circ\text{C}$.

These observations lead to the following rate expression, evidencing the first-order dependence of the rate on initial catalyst concentration and the zero-order dependence on substrate concentration:

$$\text{rate} = k[\text{Pt}]_0$$

In Scheme 4 a possible reaction pathway is suggested accounting for all the above-mentioned spectroscopic and kinetic evidence. The catalyst coordinates the alkene, which becomes electron poor and induces the migration of the C_6F_5 residue, leading to overall insertion of the alkene and formation of Pt-alkyl species. The latter is then subjected to β -hydride elimination with formation of diphosphine Pt-hydride and release of a pentafluoro phenyl vinyl byproduct (seen by GC-MS). These initial steps account for the formation of the actual catalyst and justify the induction time. The same Pt-H species is obtained independently of the alkyl/aryl ligand present on the metal, albeit with different rates (see above). The produced hydride is coordinatively unsaturated and promptly reacts with the alkene followed by rapid hydride migration to the double bond and formation of a Pt-alkyl species that is constrained by the large bite angle²⁴ of dppb, eventually showing the agostic interaction.²⁵ Here we can distinguish two possible agostic intermediates: one arising from hydride attack to the alkene C^2 and formation of an unproductive agostic intermediate A and one derived by hydride attack to C^1 leading to species B. The latter slowly transforms into species C (the rate-determining step) by dissociation of the weak agostic interaction followed by rotation around the Pt-C bond and formation of a new agostic contact with a hydrogen bound to C^3 . Species C undergoes β -hydride elimination and formation of Pt-H species and the isomerized alkene, which is quickly replaced by the incoming terminal alkene that binds more strongly to Pt^{II} complexes.²⁶ Through *ab initio* and DFT calculations applied to $\text{Pt}(\text{PR}_3)_2(\text{H})(\text{propene})^+$ complexes ($\text{R} = \text{H}, \text{F}, \text{CH}_3$) Creve et al. demonstrated that insertion of the alkene in

(24) Dierkes, P.; van Leeuwen, P. W. N. M. *J. Chem. Soc., Dalton Trans.* **1999**, 1519–1529.

(25) Mole, L.; Spencer, J. L.; Carr, N.; Orpen, A. G. *Organometallics* **1991**, *10*, 49–52.

(26) (a) Crabtree R. H. *The Organometallic Chemistry of the Transition Metals*; John Wiley & Sons: New York, 1988. (b) Collman J. P.; Hegedus L. S.; Norton J. T.; Finke R. G. *Principles and Applications of Organotransition Metal Chemistry*; University Science Books: Mill Valley, CA, 1987.

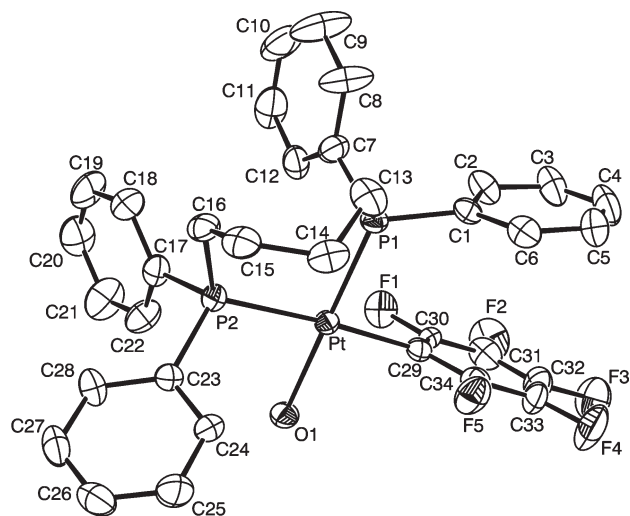
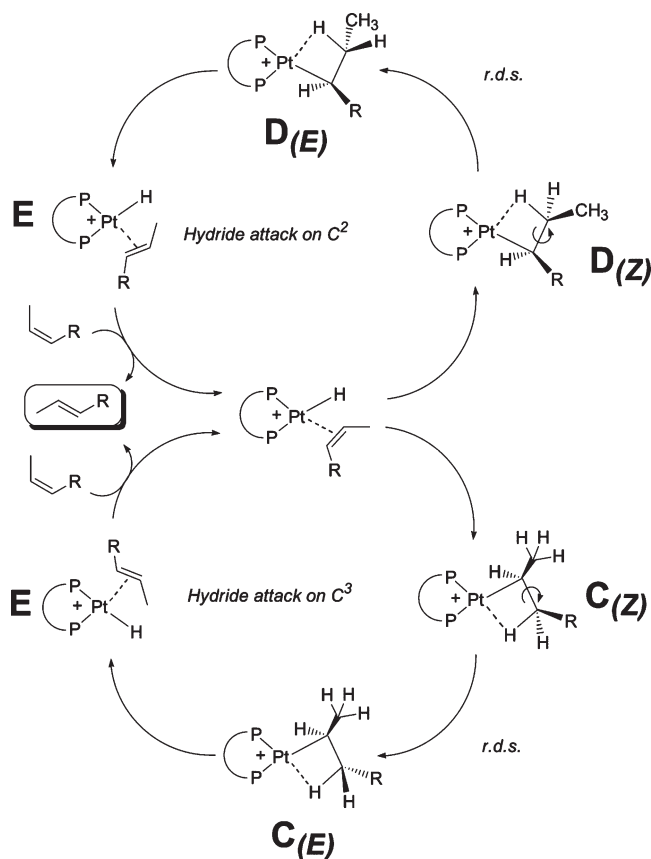


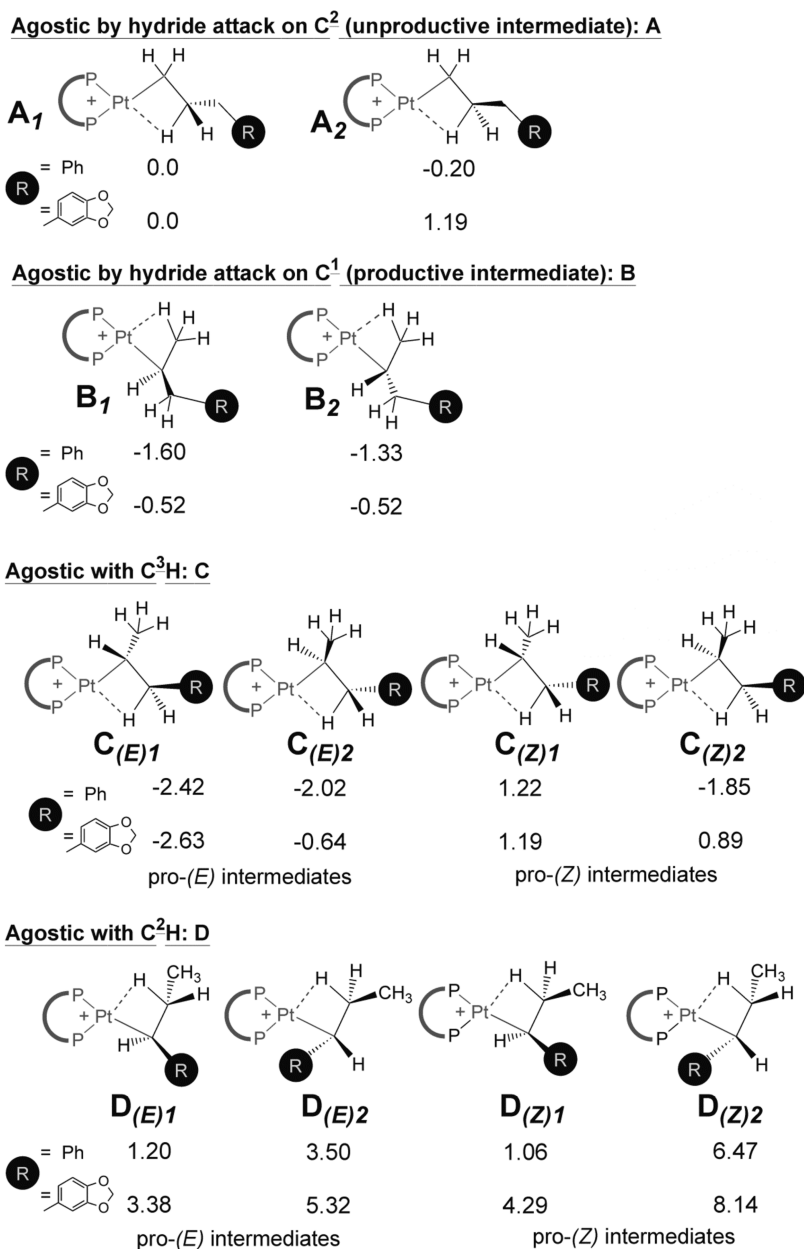
Figure 4. ORTEP drawing of the cationic portion of the complex $\text{cis}-[(\text{dppb})\text{Pt}(\text{C}_6\text{F}_5)(\text{H}_2\text{O})] \cdot \text{SO}_3\text{CF}_3 \cdot \text{H}_2\text{O}$. Selected bond lengths (\AA) and angles (deg): Pt–P(1) 2.212(3), Pt–C(29) 2.059(9), Pt–P(2) 2.312(3), Pt–O(1) 2.139(6); P(1)–Pt–P(2) 93.8(1), C(29)–Pt–O(1) 87.2(3), C(29)–Pt–P(1) 90.9(3), O(1)–Pt–P(2) 88.1(2), O(1)–Pt–P(1) 176.7(2), C(29)–Pt–P(2) 175.1(3).

Scheme 5. Proposed Isomerization Pathway for *Z* to *E* Alkene Interconversion



the Pt-H bond and β -elimination processes are characterized by small activation barriers, up to 2.4 kcal/mol. Moreover the same study underlined the preference for hydride migration to C^2 , leading to linear alkyl complexes, rather

Scheme 6. Energy Values for Minimized Agostic Species A–D Involved in Schemes 4 and 5



than attack on C¹, which provides branched Pt-alkyl species.²⁷ This general view is consistent with the rate law and the spectroscopic and reactivity data reported above and with the essential features of the classical 1,2-hydrogen shift mechanism shown in Scheme 1A.

On this basis, the slow step of the reaction is suggested to be the transformation of species B into C, where the Pt^{II} metal center releases the agostic interaction with C¹-H and after rotation around the Pt-alkyl bond it makes agostic contact with C³-H. Experimental evidence based on NMR dynamic experiments on a Pd^{II} complex bearing an isopropyl residue with a Pt···H agostic interaction demonstrated that such rotation can have activation barriers as high as ca. 9 kcal/mol.²⁸ As a consequence, initial *E/Z* selectivity

observed experimentally in this work (Figure 1A) arises from kinetic control of the transformation of B into the two possible C species, one where the alkyl residue with agostic interaction is *pro-E* and one *pro-Z*.

What pushes the selectivity toward the *E* isomer approaching thermodynamic equilibrium in the case of complex **4e** and similar species is a consecutive isomerization of the (*Z*)-2-alkene when the concentration of the starting substrate approaches zero (Figure 1). Preferential coordination of the (*Z*)-2-alkene is favored by the steric hindrance present in the catalyst (Table 1) and helps to increase the selectivity of the process toward the *E* isomer. As depicted in Scheme 5, the *Z* alkene recoordinates to Pt-H species, favored by reduced steric requirements, and hydride attack to the alkene occurs. Two possible pathways are now present depending on attack to C³ or C². In the first case an agostic interaction occurs with C²-H (C_(Z)), and its equilibration with the analogous C_(E) occurs by simple interchange of an agostic

(27) Creve, S.; Oevering, H.; Coussens, B. B. *Organometallics* **1999**, *18*, 1967–1978.

(28) Tempel, D. J.; Brookhart, M. *Organometallics* **1998**, *17*, 2290–2296.

interaction between methylene C² hydrogens, which requires a simple small rotation of the C²–C³ bond of the reagent. The more stable C_(E) species then converts to Pt–H species with an *E*-coordinated alkene, which is displaced by an incoming *Z* alkene. A similar process is possible from the original Pt–H species if attack of the hydride occurs on C² (Scheme 5). In agreement with this view is also the solvent effect exhibited in Table 2. Where competition exists with more coordinating solvents, enrichment in the *E* isomer via consecutive coordination of the (*Z*)-2-alkene becomes more and more difficult. However, where the steric hindrance of the (*Z*)-2-alkene is not compatible with the steric congestion of the catalyst (i.e., with 3,4-dimethoxyallylbenzene, eugenol, and safrole as substrates) the first isomerization process is much slower and the consecutive *Z* to *E* interconversion becomes negligible, leaving the selectivity unaffected.

Crystal Structure Determination of 4e and DFT Calculations on Possible Intermediates. In order to substantiate the reaction pathways reported in Schemes 4 and 5 and shed light on the nature of the Pt···H agostic intermediates present as resting states in the catalytic cycle, several unsuccessful attempts were made to crystallize such species out of the reaction mixture. Nevertheless, a reliable starting point concerning ligand conformation was obtained from crystals of **4e** grown from dichloromethane/hexane, whose structure was solved (Figure 4). An interesting and somehow unexpected feature is the –(CH₂)₄– alkyl chain being not puckered but completely above (or below) the coordination plane. This positions two aromatic rings of the ligand pointing almost perpendicularly under the coordination plane, while the other two remain in equatorial position, acting as arms that limit the space occupied by the perfluoro-aromatic moiety and water. The value found for the P₁–Pt–P₂ bite angle (93°) is in line with that proposed by van Leeuwen for dppb in Rh complexes^{1,29} and is sufficiently large to induce agostic interactions in the catalytically active Pt^{II} species.

With these geometrical data as a starting point for energy minimizations, we performed a series of DFT calculations aiming at comparing the energies of the different agostic intermediates³⁰ A, B, C, and D (Scheme 6) to find support for the mechanisms reported above (Schemes 4 and 5).

Comparison between agostic species A and B derived from allylbenzene shows that B is more stable by about 1 to 1.5 kcal/mol, while the energy difference is about half for the more sterically demanding safrole. Both species are present in the catalytic cycle before the rate-determining step, and the calculated energies are in agreement with the experimental spectroscopic observation of only one agostic species being practically seen for allylbenzene (B) and two for safrole and other disubstituted allylbenzene derivatives (A and B with small energy differences) as reported in Figure 2. In principle, an energy difference of 1 kcal gives rise to an isomer population of ~83:17, likely leading to the possibility to practically observe spectroscopically only one species. Further comparison of the energies for species C and D shows that the latter are generally less stable as expected considering that the aromatic residue in D is closer to the aromatic rings of the chelating diphosphine, while in C species it is placed on an opposite position with respect to the Pt atom. This observation supports a *Z* to *E* consecutive

isomerization process that occurs through coordination of the *Z* alkene to Pt and hydride attack on C³ rather than on C², leading to C_Z agostic species that are in thermodynamic equilibrium with C_E. Calculations provided also quantitative support to the preferred coordination of the Pt-hydride species, derived by elimination of the fluorinated alkene, to terminal alkene, followed by *Z* and eventually by *E* products. In fact, binding energies calculated for the three possible alkenes are terminal –18.74, *Z* –16.54, and *E* –15.00 kcal/mol, in agreement with the selectivity profile observed experimentally during the reaction progress (Figure 1).

Conclusion

The catalytic system here reported has the potential to be a viable protocol for the synthesis of a variety of fragrances via the catalytic isomerization of the corresponding terminal alkenes, as it shows good yields within hours and, in some cases, excellent *E/Z* selectivities with low (< 1% mol) catalyst loading under mild experimental conditions, in air and with ordinary solvents. In particular the results observed in the isomerization of estragole (99% yield, *E/Z* 97:3) at 50 °C in 12 h are, to our knowledge, the best thus far reported in terms of overall activity and selectivity under the mildest experimental conditions. It is worth noting that despite the well-known affinity of Pt^{II} complexes for terminal alkenes, this is the first example of an isomerization reaction catalyzed by this transition metal. Moreover a pathway involving agostic species has been clearly identified here for the first time as demonstrated by ³¹P investigation. This is made possible by the existence of unusual sterically hindered Pt^{II}-alkyl species capable of making the agostic Pt···H interchange the slow step of the isomerization process and by the moderate aptitude of this metal to promote β-hydride elimination with respect to other transition metal centers such as Rh, Ru, Pd, or Ni. Although obvious intermediates in classical 1,2-hydrogen shift via hydride addition/elimination involving β-hydride elimination, agostic species in isomerization have never been identified before.

Examples of asymmetric isomerization of simple alkenes are rare,³¹ while only a few more data are available for isomerization of double bonds close to functional groups (i.e., allylic alcohols).³² The very high selectivity toward the *E* alkene observed with the present system in some cases relies mainly on a consecutive process allowing only the *Z* alkene to enter the coordination sphere of the catalyst and be converted into the *E* isomer. The strong ligand effect on catalytic activity and product selectivity observed with complexes **4** augurs well for the development of an asymmetric version of the Pt^{II}-catalyzed alkene isomerization, which is currently underway in our laboratory.

Experimental Section

Reagents and Materials. General Procedures. ¹H NMR and ³¹P{¹H} NMR spectra were recorded at 298 K, unless otherwise stated, on a Bruker AVANCE 300 spectrometer operating at 300.15 and 121.50 MHz, respectively. δ values in ppm are relative to SiMe₄ and 85% H₃PO₄. ¹⁹F{¹H} NMR spectra were

(31) Chen, Z.; Halterman, R. L. *J. Am. Chem. Soc.* **1992**, *114*, 2276–2277.

(32) (a) Tanaka, K.; Qiao, S.; Tobisu, M.; Lo, M. M.-C.; Fu, G. C. *J. Am. Chem. Soc.* **2000**, *122*, 9870–9871. (b) Tanaka, K.; Fu, G. C. *J. Org. Chem.* **2001**, *66*, 8177–8186.

(29) (a) Sakakura, T. *J. Organomet. Chem.* **1984**, *267*, 171.

(b) Abatjoglou, A. G.; Billig, E.; Bryant, D. R. *Organometallics* **1984**, *3*, 923.

(30) Lein, M. *Coord. Chem. Rev.* **2009**, *253*, 625–634.

recorded at 298 K on a Bruker AC200 spectrometer operating at 188.25 MHz. δ values in ppm are relative to CFCl_3 . All reactions were monitored by ^1H NMR.

Substrates. All alkenes used as substrates are commercial products (Aldrich) and were used without further purification.

Synthesis of the Complexes. All work was carried out with the exclusion of atmospheric oxygen under a dinitrogen atmosphere using standard Schlenk techniques. Solvents were dried and purified according to standard methods. Substrates were purified by passing through neutral alumina and stored in the dark at low temperature. AgOTf , triphenylphosphine, and dppb were commercial products and were used without purification. The complexes $[\text{PtCl}(\text{Ph})(\text{COD})]$,³³ $[\text{Pt}(\text{C}_6\text{H}_3(\text{CF}_3)_2)_2(\text{dppe})]$,³⁴ $[\text{PtCl}(\text{Me})(\text{dppb})]$,³⁵ $[\text{PtCl}(\text{CF}_3)(\text{dppb})]$,³⁶ $[\text{PtCl}(\text{C}_6\text{F}_5)(\text{PPh}_3)_2]$,³⁷ $[\text{Pt}(\text{C}_6\text{F}_5)(\text{OH}_2)(\text{P-P})](\text{OTf})$ (with $\text{P-P} = \text{dppm}$ **4a**, dppe **4b**, (*S,S*)-chiraphos **4c**, dppp **4d**, and dppb **4e**),¹⁷ $[\text{Pd}(\text{C}_6\text{F}_5)(\text{OH}_2)(\text{dppe})](\text{OTf})$ (**4b-Pd**),³⁸ and $[\text{Pt}(\text{dppb}(\text{OH}))_2(\text{BF}_4)_2]$ ³⁹ (**7**) were synthesized following procedures reported in the literature. Elemental analyses were performed at the Department of Analytical, Inorganic and Organometallic Chemistry of the Università di Padova.

New Complexes. **[Pt(Me)(OH₂)(dppb)](OTf), 1.** To a solution of $[\text{PtCl}(\text{Me})(\text{dppb})]$ (0.16 g, 0.24 mmol) in wet dichloromethane (30 mL) was added 0.54 mL of an acetone solution of AgOTf (0.25 mmol). The suspension was stirred for 2 h; then the solid AgCl was filtered off, and the solution was concentrated. Upon treatment with *n*-hexane, a white solid was obtained, filtered off, and dried under vacuum. Yield: 0.12 g, 61.2%. Anal. Calcd for $\text{C}_{30}\text{H}_{33}\text{F}_3\text{O}_4\text{P}_2\text{PtS}$: C, 44.83; H, 4.14; S, 3.99. Found: C, 44.39; H, 4.29; S, 3.87. ^1H NMR (δ , acetone-*d*₆): 7.55–7.91 (m, Ar), 1.59 (m, CH_2), 2.03 (m, CH_2), 2.80 (m, CH_2), 3.07 (m, CH_2), 0.29 (m, $^2J_{\text{Pt-H}} = 49$ Hz, $^3J_{\text{cis-P-H}} = 2$ Hz, $^3J_{\text{trans-P-H}} = 7$ Hz, CH_3). $^{31}\text{P}\{^1\text{H}\}$ NMR (δ , acetone-*d*₆): 30.20 (m, $^1J_{\text{Pt-P}} = 1849$ Hz, $^2J_{\text{P-P}} = 14$ Hz, $\text{P}_{\text{C-trans}}$); 12.00 (m, $^1J_{\text{Pt-P}} = 4651$ Hz, $^2J_{\text{P-P}} = 14$ Hz, $\text{P}_{\text{O-trans}}$). $^{19}\text{F}\{^1\text{H}\}$ NMR (δ , acetone-*d*₆): -80.68 (s, OTf).

[Pt(CF₃)(OH₂)(dppb)](OTf), 2. The complex was synthesized as for **1** starting from $[\text{PtCl}(\text{CF}_3)(\text{dppb})]$ (0.15 g, 0.21 mmol) and 0.46 mL of an acetone solution of AgOTf (0.21 mmol). Yield: 0.10 g, 57.8%. Anal. Calcd for $\text{C}_{30}\text{H}_{30}\text{F}_6\text{O}_4\text{P}_2\text{PtS}$: C, 42.01; H, 3.53; S, 3.74. Found: C, 42.12; H, 3.39; S, 3.87. ^1H NMR (δ , acetone-*d*₆): 7.58–8.02 (m, Ar), 3.16 (m, CH_2), 2.83 (m, CH_2), 2.10 (m, CH_2), 1.63 (m, CH_2). $^{31}\text{P}\{^1\text{H}\}$ NMR (δ , acetone-*d*₆): 19.29 (m, $^1J_{\text{Pt-P}} = 1904$ Hz, $^3J_{\text{F-P}} = 55$ Hz, $^2J_{\text{P-P}} = 21$ Hz, $\text{P}_{\text{C-trans}}$); 6.09 (m, $^1J_{\text{Pt-P}} = 4321$ Hz, $\text{P}_{\text{O-trans}}$). $^{19}\text{F}\{^1\text{H}\}$ NMR (δ , acetone-*d*₆): -30.76 (dd, $^2J_{\text{Pt-F}} = 483$ Hz, $^3J_{\text{cis-P-F}} = 8$ Hz, $^3J_{\text{trans-P-F}} = 55$ Hz, CF_3), -80.61 (s, OTf).

[PtCl(Ph)(dppb)]. To a solution of $[\text{PtCl}(\text{Ph})(\text{cod})]$ (0.10 g, 0.12 mmol) in dichloromethane (20 mL) at room temperature was added 0.11 g (0.25 mmol) of dppb . The solution was stirred for 1 h, then was concentrated and treated with *n*-hexane, giving a white solid, which was filtered off, washed with hexane, and dried under vacuum. Yield: 0.16 g, 92.3%. Anal. Calcd for $\text{C}_{34}\text{H}_{33}\text{ClP}_2\text{Pt}$: C, 55.63; H, 4.53. Found: C, 55.67; H, 4.42. ^1H NMR (δ , CD_2Cl_2): 6.51–7.80 (m, Ar), 2.69 (m, CH_2), 2.37 (m, CH_2), 2.00 (m, CH_2), 1.59 (m, CH_2). $^{31}\text{P}\{^1\text{H}\}$ NMR (δ , CD_2Cl_2): 17.51 (m, $^1J_{\text{Pt-P}} = 4293$ Hz, $^2J_{\text{P-P}} = 17$ Hz, $\text{P}_{\text{Cl-trans}}$), 9.09 (m,

$^1J_{\text{Pt-P}} = 1581$ Hz, $^2J_{\text{P-P}} = 17$ Hz, $\text{P}_{\text{C-trans}}$). FT-IR (ν , CsI): 283.34 (Pt-Cl str.).

[Pt(Ph)(OH₂)(dppb)](OTf), 3. The procedure is similar to that followed for complex **1** starting from $[\text{PtCl}(\text{Ph})(\text{dppb})]$ (0.14 g, 0.19 mmol) and 0.43 mL of an acetone solution of AgOTf (0.20 mmol). Yield: 0.12 g, 80.7%. Anal. Calcd for $\text{C}_{35}\text{H}_{35}\text{F}_3\text{O}_4\text{P}_2\text{PtS}$: C, 48.56; H, 4.07; S, 3.70. Found: C, 48.39; H, 3.89; S, 3.87. ^1H NMR (δ , acetone-*d*₆): 6.62–7.91 (m, Ar), 3.12 (m, CH_2), 3.00 (m, CH_2), 1.93 (m, CH_2), 1.60 (m, CH_2). $^{31}\text{P}\{^1\text{H}\}$ NMR (δ , acetone-*d*₆): 24.55 (d, $^1J_{\text{Pt-P}} = 1757$ Hz, $^2J_{\text{P-P}} = 14$ Hz, $\text{P}_{\text{C-trans}}$); 8.41 (d, $^1J_{\text{Pt-P}} = 4654$ Hz, $^2J_{\text{P-P}} = 14$ Hz, $\text{P}_{\text{O-trans}}$). $^{19}\text{F}\{^1\text{H}\}$ NMR (δ , acetone-*d*₆): -80.66 (s, OTf).

[Pt(C₆F₅)(OH₂)(PPh₃)₂](OTf), 5. To a solution of $[\text{PtCl}(\text{C}_6\text{F}_5)(\text{PPh}_3)_2]$ (0.13 g, 0.14 mmol) in wet dichloromethane (20 mL) and acetone (5 mL) at room temperature was added 0.35 mL of an acetone solution of AgOTf (0.16 mmol). The suspension was stirred overnight; then the solid AgCl was filtered off and the solution was concentrated. Upon treatment with diethyl ether, a white solid was obtained, filtered off, and dried under vacuum. Yield: 0.13 g, 86.3%. Anal. Calcd for $\text{C}_{43}\text{H}_{32}\text{F}_8\text{O}_4\text{P}_2\text{PtS}$: C, 49.01; H, 3.06. Found: C, 48.97; H, 3.02. ^1H NMR (δ , CDCl_3): 7.30–7.55 (m, Ar). $^{31}\text{P}\{^1\text{H}\}$ NMR (δ , CDCl_3): 22.28 (m, $^1J_{\text{Pt-P}} = 2721$ Hz); $^{19}\text{F}\{^1\text{H}\}$ NMR (δ , CDCl_3): -80.88 (s, OTf), -122.55 (d, $^3J_{\text{Pt-F}} = 427$ Hz, $^3J_{\text{F-F}} = 22$ Hz, *o*-F), -165.62 (t, $^2J_{\text{F-F}} = 20$ Hz, *p*-F), -166.85 (m, *m*-F).

[PtCl(C₆H₃(*m,m*-CF₃)₂)(dppe)]. To a solution of $[\text{Pt}(\text{C}_6\text{H}_3(\text{CF}_3)_2)_2(\text{dppe})]$ (0.20 g, 0.20 mmol) in dichloromethane (20 mL) and methanol (5 mL) was added 0.015 mL of acetyl chloride (0.20 mmol). The solution was stirred overnight and then concentrated. The product was purified by chromatography on silica gel (diethyl ether/*n*-hexane, 9:2, $R_f = 0.49$). Yield: 0.11 g, 66.6%. Anal. Calcd for $\text{C}_{34}\text{H}_{27}\text{ClF}_6\text{P}_2\text{Pt}$: C, 48.50; H, 3.23. Found: C, 48.39; H, 3.29. ^1H NMR (δ , CDCl_3): 7.20–7.97 (m, Ar), 2.49 (m, CH_2), 2.22 (m, CH_2). $^{31}\text{P}\{^1\text{H}\}$ NMR (δ , CDCl_3): 40.43 (s, $^1J_{\text{Pt-P}} = 1765$ Hz, $\text{P}_{\text{C-trans}}$), 39.63 (s, $^1J_{\text{Pt-P}} = 3996$ Hz, $\text{P}_{\text{O-trans}}$). $^{19}\text{F}\{^1\text{H}\}$ NMR (δ , CDCl_3): -65.40 (s, CF_3).

[Pt(C₆H₃(*m,m*-CF₃)₂)(OH₂)(dppe)](OTf), 6. The complex was synthesized as for **1** starting from $[\text{PtCl}(\text{C}_6\text{H}_3(\text{CF}_3)_2)_2(\text{dppe})]$ (0.065 g, 0.072 mmol) and 0.17 mL of an acetone solution of AgOTf (0.079 mmol). Yield: 0.059 g, 78.4%. Anal. Calcd for $\text{C}_{35}\text{H}_{29}\text{F}_9\text{O}_4\text{P}_2\text{PtS}$: C, 43.17; H, 3.00; S, 3.29. Found: C, 43.39; H, 2.89; S, 3.37. ^1H NMR (δ , acetone-*d*₆): 7.35–8.01 (m, Ar), 2.97 (m, CH_2), 2.66 (m, CH_2). $^{31}\text{P}\{^1\text{H}\}$ NMR (δ , acetone-*d*₆): 49.87 (s, $^1J_{\text{Pt-P}} = 1863$ Hz, $\text{P}_{\text{C-trans}}$), 33.15 (s, $^1J_{\text{Pt-P}} = 4385$ Hz, $\text{P}_{\text{O-trans}}$). $^{19}\text{F}\{^1\text{H}\}$ NMR (δ , acetone-*d*₆): -65.12 (s, CF_3), -80.58 (s, OTf).

Isomerization Reactions. These were carried out in air in a 2 mL vial equipped with a screw-capped silicone septum to allow sampling. Stirring was performed by a Teflon-coated bar driven externally by a magnetic stirrer (700 rpm). Constant temperature was maintained by water or alcohol circulation through an external jacket connected with a thermostat. Typically, the proper amount of catalyst (0.016 mmol, 2% mol) was placed in the vial, followed by the solvent (1.0 mL); subsequently the vial was thermostated. After stirring for 10 min, the substrate (0.83 mmol) was added and time was started. All reactions were monitored by GC analysis and ^1H NMR by periodically sampling directly from the reaction mixtures with a microsyringe. Quenching of the samples by adding an excess of LiCl was performed prior to NMR analysis.

Computational Details. The calculations were performed with the ADF2007.1⁴⁰ package at the BLYP⁴¹ level using the

(33) Clark, H. C.; Manzer, L. E. *J. Organomet. Chem.* **1973**, *59*, 411–428.

(34) Eaborn, C.; Odell, K. J.; Pidcock, A. *J. Chem. Soc., Dalton Trans.* **1978**, 357–368.

(35) Romeo, R.; D'Amico, G. *Organometallics* **2006**, *25*, 3435–3446.

(36) Zanardo, A.; Michelin, R. A.; Pinna, F.; Strukul, G. *Inorg. Chem.* **1989**, *28*, 1648–1653.

(37) Al-Fawaz, A.; Aldridge, S.; Coombs, D. L.; Dickinson, A. A.; Willock, D. J.; Ooi, L.-L.; Light, M. E.; Coles, S. J.; Hursthouse, M. B. *J. Chem. Soc., Dalton Trans.* **2004**, 4030–4037.

(38) Casado, A. L.; Espinet, P.; Gallego, A. M.; Martínez-Illarduya, J. M. *Chem. Commun.* **2001**, 339–340.

(39) Gavagnin, R.; Cataldo, M.; Pinna, F.; Strukul, G. *Organometallics* **1998**, *17*, 661–667.

(40) (a) te Velde, G.; Bickelhaupt, F. M.; van Gisbergen, S. J. A.; Fonseca Guerra, C.; Baerends, E. J.; Snijders, J. G.; Ziegler, T. Chemistry with ADF. *J. Comput. Chem.* **2001**, *22*, 931–967. (b) Fonseca Guerra, C.; Snijders, J. G.; te Velde, G.; Baerends, E. J. *Theor. Chem. Acc.* **1998**, *99*, 391. (c) ADF2007.01, SCM, Theoretical Chemistry; Vrije Universiteit: Amsterdam, The Netherlands, <http://www.scm.com>.

(41) (a) Becke, A. D. *Phys. Rev. A* **1988**, *38*, 3098–3100. (b) Lee, C.; Yang, W.; Parr, R. G. *Phys. Rev. B* **1988**, *37*, 785–789.

TZ2P basis set in the frozen core approximation. Scalar relativistic effects were taken into account by the zeroth-order regular approximation (ZORA).⁴² The geometry optimizations were performed without any symmetry constraint, followed by analytical frequency calculations to confirm that a minimum had been reached. Cartesian coordinates and energies of stationary points are reported in the Supporting Information.

(42) Van Lenthe, E.; Baerends, E. J.; Snijders, J. G. *J. Chem. Phys.* **1994**, *101*, 9783.

Acknowledgment. The authors thank MIUR, Università Ca' Foscari di Venezia, and Università degli Studi di Padova for financial support. G.S. thanks Johnson-Matthey for the loan of platinum. L. Sporni is gratefully acknowledged for GC-MS analysis.

Supporting Information Available: Molecular modeling coordinates for agostic species A–D and the alkene isomers reported in Table 4 are reported together with a cif file for complex **4e**. This material is available free of charge via the Internet at <http://pubs.acs.org>.